JOURNAL OF MATERIALS SCIENCE 25 (1990) 3806–3813

In situ spectroscopic study of the electropolymerization and properties of polyterthiophene

R.M. EALES, A.R. HILLMAN*
School of Chemistry, University of Bristol, Bristol BS8 1TS, UK

The electrochemical polymerization of terthiophene has been studied using time resolved *in situ* UV–visible transmission spectroscopy. The similarity of monomer and polymer oxidation potentials allows one to deposit partially or fully doped polymer. Both coulometric and spectroscopic data show that the level of doping increases with polymerization potential up to about 1.1 V, at which point it attains its maximum value of one positive charge per four rings, as for the parent thiophene. At the relatively low polymerization potentials employed, incompletely polymerized material is trapped within the polymer film. Direct evidence for the presence of trapped monomer is the disappearance of a peak at 355 nm upon the application of positive potentials to a film transferred to monomer-free background electrolyte. Spectroscopic and coulometric assay of these species shows that they constitute an appreciable fraction (ca. 20%) of the immobilized material at low polymerization potentials. The ability of these species to remain unpolymerized decreases with increasing polymerization potential. In all cases, they are polymerized during subsequent potential cycling in the range 0.0–1.15 V. The redox composition of the polymer, estimated using optical data, shows non-Nernstian behaviour.

1. Introduction

Conducting polymers are presently attracting considerable interest as a result of their rather unusual electronic and optical properties. Polymers based on acetylene, pyrrole, thiophene and aniline (together with their derivatives) have received the greatest attention. Reviews of these materials and areas of potential application have appeared in [1] and elsewhere [2–5].

The polymers we have been studying are from the thiophene series. This choice has been prompted by the facility to electrochemically control both the polymerization and "doping" processes, and by the stability of the resultant polymers. In the former instance we have explored particularly the use of polymerization potential as a control variable. In the latter instance, stability allows the use of film characterization techniques requiring prolonged sample manipulation or data acquisition.

Electrochemistry has been used to both control (via potential) and measure (via current) the rate of monomer consumption. The resultant variation of current with time has been analysed according to nucleation and growth models originally developed to describe the electrodeposition of metals [6], and applied to the deposition of conducting (pyrrole-based) polymers by Pletcher *et al.* [7, 8]. Our studies extended this to thiophene (T) [9] and bithiophene (BT) [10] polymerization. A limitation of this approach is that, strictly speaking, one monitors monomer consumption, rather than polymer production. This results in ambiguities (associated with the multiplicity of species involved) not encountered for the analogous metal deposition reactions.

Spectroscopic techniques, in particular UV–visible absorbance measurements [11, 12], are well suited to identification of the species involved. In our work, this has proved useful for T and BT in several respects: the transient observation of intermediates and the onset of the desirable "metallic" character during polymerization, and the equilibrium film optical properties as a function of potential (doping level) [10, 13]. In transmission mode, one views both surface and solution species. Consequently, although the technique is useful for identifying the species involved it does not reveal their location.

This issue has been addressed using ellipsometry, a reflection technique which responds primarily to surface species. We have been able to deomonstrate that the intermediates in thiophene polymerization are in solution, and to correlate the (optically determined) appearance of adsorbed material with the (electrochemically deduced) nucleation process for thiophene polymerization [14, 15]. An additional feature of the technique is that one obtains *solvated* film thickness, and can monitor film thickness changes associated with the ingress of dopant ions (and any associated solvent) during redox cycling [15].

This paper is part of a programme of work investigation the effect of starting material on final film properties for thiophenes. Simplistically, one might expect that the same polymer would result (although the potential and charge required to produce the

*To whom correspondence should be addressed.

0022–2461/90 $03.00 + .12

polymer might decrease with increasing oligomer size). This view is based on the hypothesis that the oligomers (bithiophene, terthiophene, quaterthiophene, etc.) are produced en route from thiophene to polythiophene. The experimental evidence of a number of workers shows this *not* to be the case. Optical and electrochemical properties of polymers derived from 2,2′-bithiophene (BT) [16–25], 2,2′-5′,2″-terthiophene (TT), [17, 21, 23–26] and 2,2′-5′,2″-5″,2‴-quaterthiophene (QT) [20, 24–26] differ from those of polythiophene. Unfortunately, different workers chose to use different polymerization conditions, so direct comparisons are difficult. Of particular relevance is the choice of potentiostatic [9, 16, 19], potentiodynamic [20] or galvanostatic [17, 18, 21, 23, 25] control of polymerization. We believe that the conditions of polymerization may be crucial, and have therefore chosen to study polymerization of the series T, BT, TT under potentiostatic control, as a function of the selected polymerization potential.

In addition to the interest in general trends on ascending the homologous series of thiophenes, there was a rather more special reason for studying PTT. Threshold potentials for polymerization of T, BT and TT are ca. 1.6, 1.15 and 0.98 V, respectively. Potentials required for oxidation of the resulting polymers are all ca. 1.0 V. This implies that the first two members of the series are *necessarily* deposited in their oxidized ("doped") forms. However, for TT, the similarity of polymerization and "doping" potentials results in the opportunity to deposit fully or partially doped polymer, as selected via the polymerization potential. That this is the case was demonstrated in a preliminary note [27]. The object of this paper is to quantify this effect and to investigate the extent to which the doping level during growth affects final film properties. We also point out that the facility to grow films of variable doping level allows one to study the polymerization and doping processes separately. The first part of this report describes time-resolved UV–visible spectroscopic observation of the polymerization process itself, and correlation with the simultaneously measured current. The second part concerns the characterization of the resultant films in monomer-free solution and the effects of potential cycling.

2. Experimental details

The electrochemical instrumentation has been described in detail elsewhere [9]. The potential was generated by a purpose-built variable height/variable duration pulse unit and controlled by an Oxford Electrodes potentiostat. Current transients were recorded on a Gould OS4020 digital storage oscilloscope or a Bryans 60000 series X–Y–t recorder, as appropriate to the timescale. UV–visible spectra were acquired using a Hewlett-Packard HP8451A diode array spectrophotometer, synchronized with the electrochemical instrumentation as reported previously [3].

The solvent for both polymerization and characterization experiments was CH_3CN (Analar, refluxed over CaH_2, distilled and stored over molecular sieves). The background electrolyte was 0.1 mol dm^{-3} tetraethylammonium tetrafluoroborate, TEAT (puriss., Fluka). Monomeric terthiophene (Aldrich) was shown by thin layer chromatography to contain a coloured impurity. The pure TT was separated using preparative scale TLC (on silica, with hexane/3% acetone as the eluent); the absence of higher oligomers was confirmed by comparison of UV–visible spectra with literature spectra [28].

Working electrodes for purely electrochemical experiments were stationary platinum disc electrodes of area 0.393 cm^2. For the spectroelectrochemical experiments they were gold sputtered on ultrasonically cleaned glass (visible region measurements) or quartz (measurements extending into the UV region). The exposed area of these electrodes was typically 1 cm^2, and typical electrode resistances were 10–20 Ω, so that ohmic drop problems were not serious. All potentials were measured and are quoted with respect to SCE. The counter electrode was a large platinum foil. All solutions were initially purged with argon, then the gas stream was directed over the solution during measurements to maintain quiescent solution conditions. The water content of solutions was reduced using molecular sieves, although we note that some water is inevitably present since these were not "glovebox" experiments. Measurements were made at room temperature (20° C). The potential profile consisted of a double potential step from 0 V to the polymerization potential, E_{pol}, for a time t_p, then back to 0 V. Spectral ranges and acquisition times are given with the relevant figures.

3. Results and discussion

3.1. Film growth:

3.1.1. Electrochemical data

Current responses to applied potential steps from 0 V to potentials above the polymerization threshold have been qualitatively described in a preliminary communication [27]. In all cases we see monotonically falling currents after the initial spike, with no evidence for nucleation processes at short times. This behaviour is similar to that seen for BT [10] but different to that for T [9].

When the polymerization potential is above the voltammetric peak potential for monomer oxidation ($E_{pol} > E_p = 1.1$ V at 20 mV sec^{-1}), the process is diffusionally controlled. The time dependence of the current under such circumstances is described by the Cottrell equation:

$$i = nFA(D/\pi t)^{1/2}c \qquad (1)$$

A linear i–$t^{-1/2}$ plot is diagnostic for diffusional behaviour, and the slope gives access to the monomer diffusion coefficient, D_{TT}, provided the bulk concentration of monomer, c, is known. Figure 1 shows the predicted linearity. In using the slope to calculate D_{TT}, we have used a value of $n = 2.75$ for the polymerization/doping process. In other words, we note that the doping is complete (one charge per four rings) at the upper end of the potential range [27]. This leads to a value for the diffusion coefficient of TT (in CH_3CN 0.1 mol dm^{-3} TEAT),

$$D_{TT}/\text{cm}^2\,\text{sec}^{-1} = 1.27\,(\pm 0.15) \times 10^{-5} \qquad (2)$$

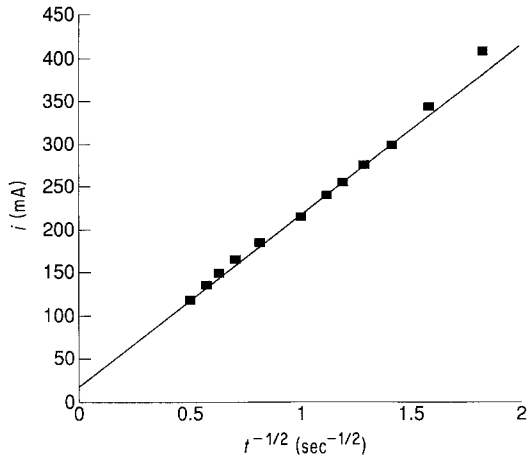

Figure 1 Cottrell plot (Equation 1) for TT (1 mmol dm^{-3}) polymerization on a platinum disc (area 0.393 cm^2) potentiostatted at 1.30 V.

which is in accord with values for similar sized aromatic hydrocarbons in CH_3CN [29].

At polymerization potentials below E_p, the process is kinetically controlled. As a measure of the rate of this process and its potential dependence, we have chosen to compare values of the current at relatively long times after the initial spike. The (approximate) independence of i on t [27] implies that growth at this point is in 1-D under kinetic control [6]. The growth law for such behaviour is [6]

$$i = nFAk' \quad (3)$$

where k' mol cm^{-2} s^{-1} is the rate constant for film growth. One would expect k', as an electrochemical rate constant, to show an exponential dependence on potential.

In treating this data, we have to take account of two effects. Firstly, we must deal with concentration polarization; the procedure here is to plot ln $(i_D/i - 1)$ (rather than ln i) as the ordinate, where i_D is the diffusionally limited current (see Equation 1). This takes account of the finite supply of reactant. Secondly, as described previously [27] and expanded below, the doping level, X, and thus the appropriate value of n $(= 2 + X)$ in Equation 1 depends on the potential. The value of X increases approximately linearly up to 0.75 (one charge per four rings) at 1.10 V [27]. Consequently, we must use nE as the ordinate, where n takes into consideration the doping level appropriate to the polymerization potential used.

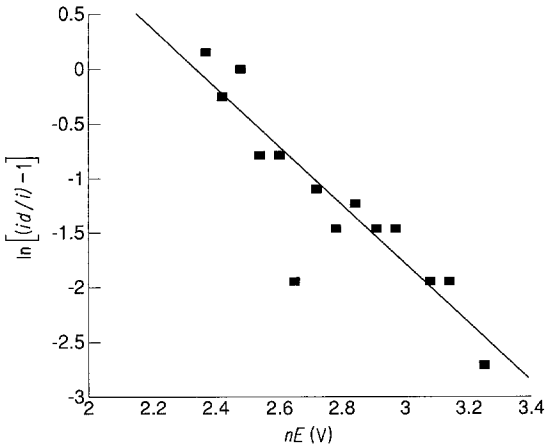

Figure 2 Tafel plot for TT (1 mmol dm^{-3}) polymerization at low polymerization potentials (< 1.1 V).

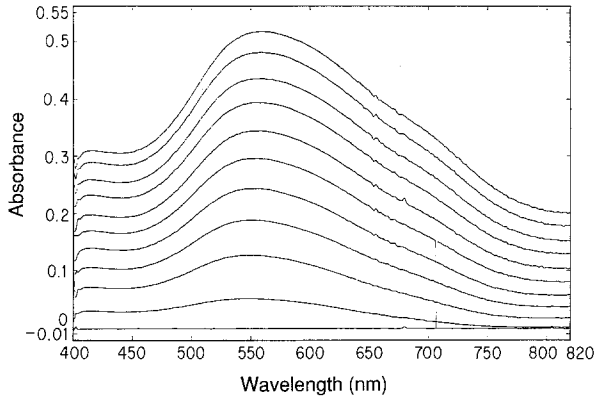

Figure 3 Spectra for PTT film growth rate at 1.06 V. Spectra were taken at 2 sec intervals but, for clarity of presentation, alternate spectra are displayed. Data analysis (see Figs 5–7) employed all spectra obtained.

Figure 2 shows such a Tafel plot for low (< 1.1 V) polymerization potentials, where the x-axis has been corrected for variable doping level and the y-axis for concentration polarization. Within experimental error, the plot is linear. The value of the transfer coefficient, $\alpha \simeq 0.06$, shows that there is little potential dependence. Converting this to a value of $\alpha n \simeq 0.17$, gives a value not dissimilar to the findings for T [9] and BT [10]. Values of k' can be obtained from the currents using Equation 3.

3.1.2. Spectroscopic data

The spectra obtained at low (E_{pol} < 1.10 V) and high (E_{pol} > 1.10 V) polymerization potentials are different; see Figs 3 and 4, respectively, and [27]. There is a progressive transition between these two types of behaviour. In all cases, there is the development of a strong band centred at 560 (± 20) nm, but the behaviour at long wavelengths depends on the polymerization potential. We consider first the common behaviour, then the differences.

The position of the band centred near 560 nm shows no systematic trend with potential over the entire range of polymerization potentials used. This implies production of this same chromophore under all conditions. In attempting to estimate the chain length of this entity, we utilize peak wavelengths of authentic α,α'-linked oligomeric thiophenes [28] (see Table I). We utilize the empirical relationship between the values of the maximum absorption wavelength (λ_{max}) and the number of linked rings (N), as has been done previously [12, 24, 25]. This is analogous to the

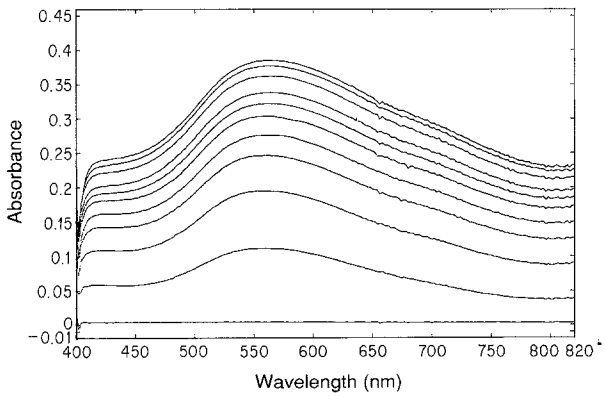

Figure 4 Analogous data to Fig. 3, for PTT film growth at 1.15 V.

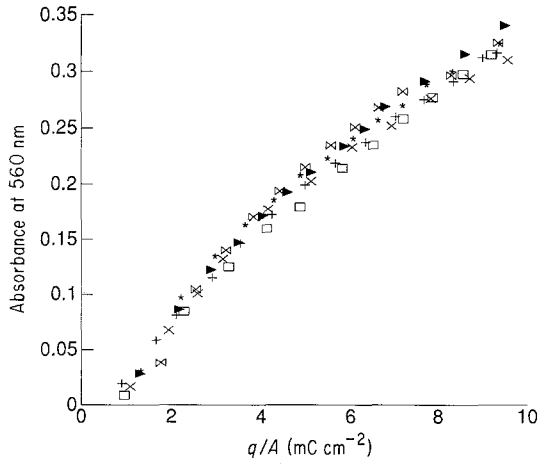

Figure 5 Absorbance against charge plots for 560 nm data, during the polymerization of TT. The polymerization potentials were 1.03 V (+), 1.07 V (■), 1.10 V (x), 1.15 V (▶), 1.20 V (*) and 1.29 V (⋈).

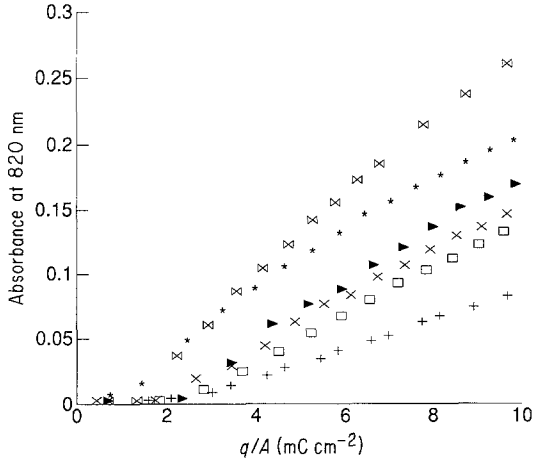

Figure 6 Absorbance against charge plots for 820 nm data, during the polymerization of TT. The polymerization potentials were 1.05 V (+), 1.08 V (□), 1.10 V (x), 1.12 V (▶), 1.17 V (*) and 1.27 V (⋈).

relationships between monomer oxidation potential, λ_{max} and N for several conjugated polymer systems [30]. A peak wavelength of 560 nm corresponds to a conjugation length (not necessarily chain length) of ca. 13 rings. This is, for reasons emphasized previously [10, 13], only an approximate guide to the extent of delocalization, particularly since the peak is very broad (fwhm = 150 nm), and is probably the result of absorption by several similar species. Nevertheless, this does give the clear indication that a chromophore containing ca. 4 monomer units is produced from the early stages of polymerization and is present throughout film depositon. These findings closely follow those for T [13] and BT [10], where the values of λ_{max} (N) were 580 nm (14 rings) and 595 nm (16 rings) respectively.

As further evidence of the independence of behaviour with polymerization potential *in this wavelength range*, we attempt to quantify the data. Our chosen form of comparison is to plot absorbance (a measure of polymer produced) against charge passed (a measure of monomer consumed). Figure 5 shows such a plot for a range of polymerization potentials covering both the kinetically and diffusionally controlled regimes. Three observations are made. The key point is that all the data fall on a common line, within experimental error. This supports the contention of the previous paragraph, and shows that the only effect of potential is to alter the rate (not efficiency) of production of this chromophore. Secondly, the plot is curved, presumably due to variation of extinction coefficient with film thickness; we have no reason to assume its constancy. Thirdly, there is an intercept on the x-axis. From its value, ca. 0.8 ($\pm$0.2) mC cm^{-2}, we deduce that ca. 4 nmol cm^{-2} of TT (12 nmol cm^{-2} of thiophene rings) are consumed before production of the chromophore. This is comparable to the 9 nmol cm^{-2} required to produce a (hypothetical, idealized) slab of material comprising 13-ring species oriented perpendicular to the electrode. In short, the quantity of species involved is consistent with oligomer, but not extensive polymer, formation at this stage.

The absorbance at 820 nm shows a more complex dependence on both polymerization potential and time. Figure 6 shows representative absorbance data at 820 nm for a set of films grown at different potentials. The first, obvious feature is that the common behaviour seen for the 560 nm data is not found. The slopes of the lines (related to extinction coefficients) are greater at higher potentials. To some extent, this is a consequence of the fact that the polymer is only fully doped (X = 0.75) for potentials above 1.10 V, and absorbance at these longer wavelengths is associated with high conductivity.

Secondly there is an intercept on the charge axis, 1.0–2.0 mC cm^{-2}, from which we can deduce that ca. 8 nmol cm^{-2} of TT are consumed before "metallic" characteristics begin to develop. This corresponds to a (hypothetical, uniform) film approximately 32-rings thick. For films grown at potentials below 1.15 V there is a linear dependence of absorbance at 820 nm on the charge passed. However, this trend is not observed until 5 mC cm^{-2} of charge has been passed. For polymerization potentials above 1.15V the plots curve over suggesting that the film is being damaged, as it is grown, by the relatively high potential. Extinction coefficients at 820 nm for PTT were found to lie in the same region as those for PBT, 0.25 – 0.60 × 10^7 cm^2 mol^{-1}.

The absorbance at 560 nm is proportional to the total amount of polymer whereas the absorbance at 820 nm is related to that fraction of the polymer

TABLE I Absorption maxima in the UV–visible region for oligomeric α, α′-linked thiophenes*

Species	Abbreviation	λ_{max} (nm)
Thiophene	T	231
2,2′-bithiophene	BT	305
2,2′-5′, 2″-terthiophene	TT	355
2,2′-5′, 2″-5″, 2‴-quaterthiophene	QT	391
2,2′-5′, 2″-5″, 2‴-5‴, 2⁗-quinquethiophene	QiT	416

*Data from [24] and [28].

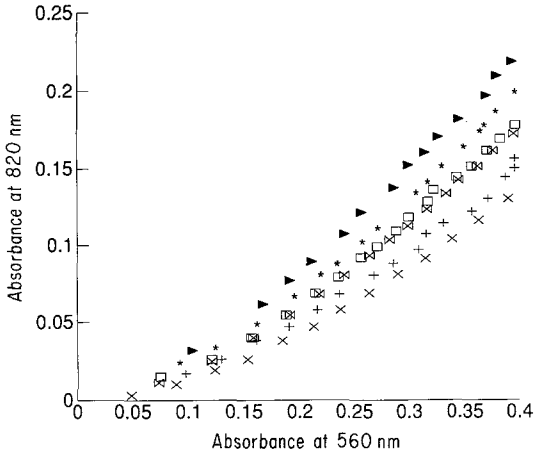

Figure 7 Comparison of absorbances at 820 and 560 nm. The polymerization potentials were 1.05 V (+), 1.06 V (x), 1.07 V (□), 1.08 V (⋈), 1.10 V (*) and 1.12 V (▶).

exhibiting metallic properties. Figure 7 shows that these two are not linearly related. The plots have an intercept on the x-axis (absorbance at 560 nm) of 0.04, representing the amount of bulk polymer that must be laid down before the onset of "metallic" properties. However, once the initial layer has been deposited the absorbance at 820 nm increases more quickly that that at 560 nm. The gradient of the plots increases with polymerization potential, indicating that "metallic" properties develop more rapidly with film thickness at higher potentials.

3.2. Film properties

Preformed PTT films were transferred to monomer-free background electrolyte and cycled between 0.00 V and 1.20 V. Several scans were required before reproducible behaviour was established. We therefore discuss the evolution and ultimate result of these changes separately. In all cases the changes were highlighted by presenting the data as difference spectra, referenced to the spectrum of the reduced film at the start of the voltammetric scan from 0 V.

3.2.1. Initial scans

The spectra of a reduced film before and after the first voltammetric scan were different; the absorbance between 400 and 600 nm (characteristic of reduced polymer) increased markedly, and that at 355 nm (the absorption maximum for monomeric TT) decreased. The decrease in absorbance at 355 nm was significant from ca. 1 V, the polymerization threshold. The results of a typical experiment are shown in Fig. 8. Such experiments strongly suggest that terthiophene is trapped in the film during growth and subsequently polymerized during the first potential scan. Further evidence that incompletely polymerized species are present in the film is provided by the current response on the initial anodic scan. As shown in Fig. 8c, there is a large peak in the region 1.10 V to 1.19 V, accompanied on occasions by a small shoulder at slightly more positive potentials. This large feature is associated with the polymerization of trapped oligomeric/monomeric species. The oxidation of (previously produced) polymer occurs at slightly less positive potentials, 1.05 (±0.01) V. Under certain conditions (see below) the polymerization peak is so large that the peak for polymer oxidation is obscured. Provided the potential is scanned slowly (5 mV sec^{-1}), only the peak at 1.05 V corresponding to polymer oxidation is seen on the second and subsequent scans. Here we show data for an experiment employing a scan rate of 20 mV sec^{-1}, where the second anodic scan shows both peaks. This demonstrates that we are not observing a single peak whose position is variable. In all cases, it is larger than on the inital scan, demonstrating that it is associated with the product of the species consumed at 1.10–1.19 V. We presume that trapped monomer is able to survive within the film during polymerization because the potentials employed are modest. In the case of thiophene polymerization the potentials are much more positive [13] so this phenomenon was not observed.

Data concerning the amount of terthiophene and oligomers trapped in the film are summarized in Table II. Rows 2 to 4 relate to films deposited at low, medium ($E_{pol} \simeq E_{pol}$ = 1.1 V) and high potentials. Column 2 is the coulometrically determined quantity of polymer deposited during the potentiostatic polymerization reaction. Columns 3 and 4 relate to data from the first scan of the subsequent voltammetric experiment in background electrolyte. The additional charge passed in the anodic scan (compared to the subsequent cathodic scan) provides a coulometric estimate of trapped monomer plus oligomer ("TT + O") in column 3. (During the anodic scan the charge passed is used to polymerize trapped species as well as oxidize the film, whereas the charge passed in the cathodic scan is only associated with the polymer ("P") redox process. This difference in charges (see below) is zero after cycling.) The drop in absorbance at 355 nm is used to provide the spectroscopic estimate of trapped monomer, polymerized in this subsequent cycle, in column 4. The ratio of the numbers in columns 3 and 2 (in column 5) is the fraction of immobilized material which is incompletely polymerized. As one might expect, higher potentials result in more complete polymerization. Column 6 is generated by the data in columns 4 and 3; it is that fraction of the trapped incompletely polymerized species which is monomer. Again the extent of polymerization increases with potential.

TABLE II The amounts of monomer (TT) and short chain oligomers (O) trapped in the film during polymerization in relation to the amount of polymer (P) originally deposited

E_{pol} (V)	P (nmol cm^{-2})	TT + O (nmol cm^{-2})	TT (nmol cm^{-2})	$\frac{TT + O}{P}$	$\frac{TT}{TT + O}$
1.049	25	5.5	2.7	0.22	0.49
1.108	36	5.6	2.1	0.16	0.38
1.150	44	6.6	1.3	0.15	0.20

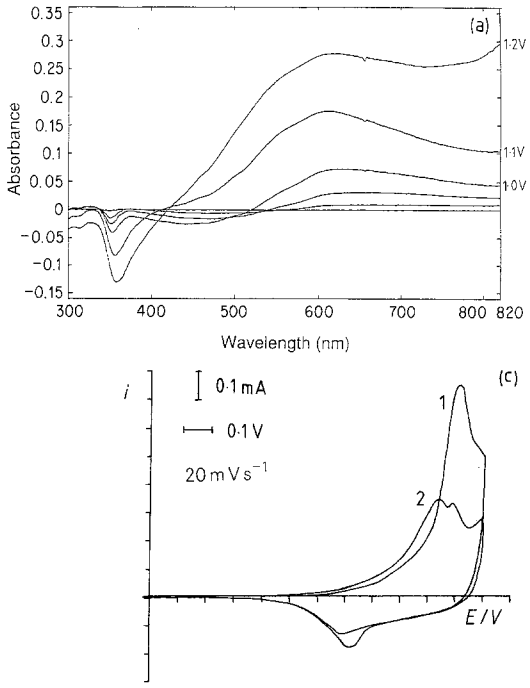

3.2.2. Final properties

On scanning positively from 0 V the absorbance was linearly dependent on the amount of charge passed, Fig. 9, up to 1.10 V. Beyond this potential the absorbance increased less than proportionately. Two obvious possibilities for this non-linearity exist. Either the optical parameters (extinction coefficients) vary with doping level or the charge is not entirely faradaic. We do not have unequivocal evidence for either, but believe the problem lies with the charge. There is a literature precedent for this assumption [31] and our data (see below) are compatible with that of others [32–34] for related materials.

The basic assumption [31] is that the porous structure of the polymer results in a very large double layer capacitance. Consequently, as the film is oxidized, extra charge is required in order to charge the double layer. At sufficiently positive potentials, the film redox process in complete, and the faradaic component of the charge is negligible. We can therefore estimate the value of the capacitance from the (now entirely capacitive) charging current. The capacitances of our PTT films calculated in this way were ca. 500 F cm^{-3},

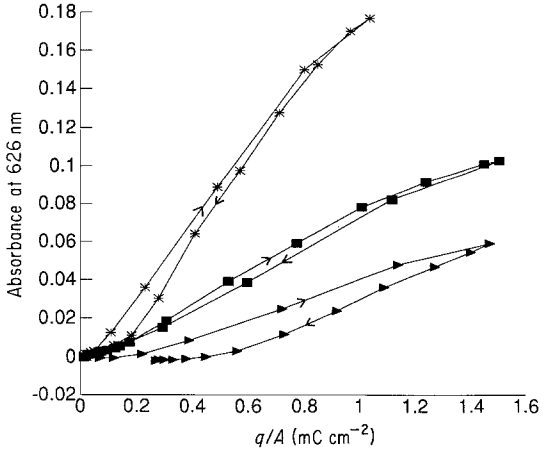

Figure 9 Absorbance (at 626 nm) against charge plots for PTT films during voltammetric experiments in background electrolyte. The polymerization potentials were 1.05 V (*), 1.11 V (■) and 1.15 V (▶).

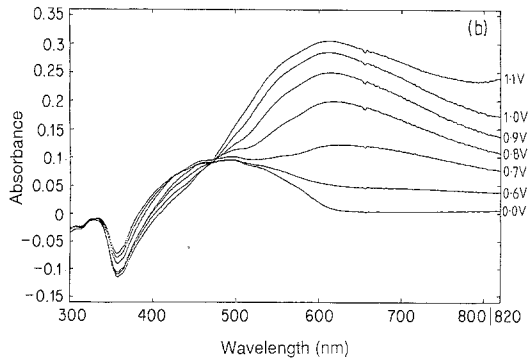

Figure 8 Spectra taken during the first voltammetric scan of a PTT film (deposited at 1.05 V) after transfer to background electrolyte. The scan rate was 20 m V sec^{-1}. (a) Data for anodic scan; potentials as marked. (b) Data for cathodic scan, (c) Current–potential curves for the first and second cycles, showing the larger anodic peak on the first scan.

e.g. a capacitance of 2.5 mF cm^{-2} for a (typical) 50 nm thick film. Similar high values, in the range 100–400 F cm^{-3}, have been reported for polypyrrole films [32–34]. We note that this numerical value contains certain complexities, in that the capacitive charge was not linearly related to the faradaic charge (estimated using optical determination of film composition, as below) as a function of E during the voltammetric scan; the same is true for polypyrrole [33].

In view of the above, we use the absorbance data as a measure of polymer redox state. The selection of monitoring wavelength is made as follows. The oxidized polymer absorbs strongly at long wavelengths ($\lambda > 820$ nm), a feature associated with the "metallic" character of the film. Since this is expected to depend not only on the state of charge but also its distribution, this will not be linearly related to oxidation state. The peak absorbance for the reduced polymer is at ca. 500 nm. However, the oxidized polymer also has an appreciable absorbance at this wavelength, so this too is also unsuitable. We have chosen to use the absorbance at 626 nm as a measure of the amount of oxidized polymer present. This has two advantages: firstly, the reduced polymer does not absorb significantly at this wavelength and, secondly, the chromophore is not associated with the metallic properties of the oxidized polymer, i.e. does not appear to depend on the distribution of oxidized segments.

We test whether the film redox composition follows a "Nernstian" relationship by plotting ln (Ox/Red) against E, as shown in Fig. 10. The plots obtained were not linear, presumably a consequence of the fact that this is not a collection of independent redox centres undergoing simple electron transfer reactions. Somewhat similar observations have been made for the poly(3-methylthiophene) system [35]. Secondly, the composition/potential relationship depends on scan direction. The potentials at which the film is 50%

TABLE III Representative values of $E_{1/2}$ for films grown at a range of potentials (data from tenth voltammetric scan at 20 m V sec^{-1})

E_{pol} (V)	$E_{1/2,a}$ (V)	$E_{1/2,c}$ (V)
1.049	1.00	0.78
1.108	1.02	0.76
1.147	1.00	0.76

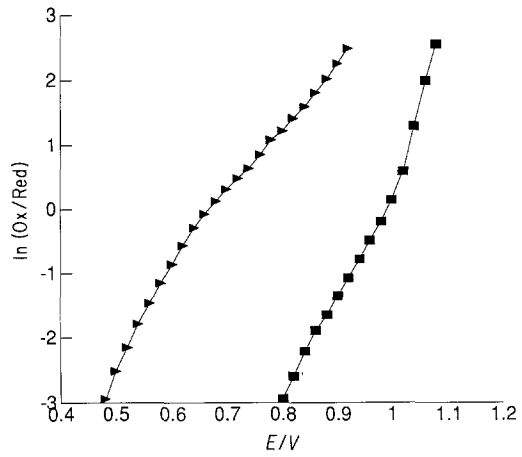

Figure 10 Plot of ln (Ox/Red) against potential ("Nernst" plot) for a PTT film in background electrolyte. Symbols (■) and (▶) represent data acquired during anodic and cathodic scans, respectively.

oxidized during anodic and cathodic scans, $E_{1/2,a}$ and $E_{1/2,c}$, are summarized in Table III. Within experimental error the values of $E_{1/2,a}$ (1.00 ± 0.02 V) and $E_{1/2,c}$ (0.74 ± 0.10 V) are independent of polymerization potential. However, they are not identical, indicating that at least one of the processes is not at equilibrium.

In an attempt to estimate the timescale on which equilibrium might be established, we conducted two experiments in which we stepped the potential to 0.9 V (ca. $\frac{1}{2}(E_{1/2,a} + E_{1/2,c})$) from 0.0 V and 1.1 V (fully reduced and oxidized, respectively). The variation of film redox state was monitored spectrophotometrically at 626 nm. The response to the positive step was slower, implying that oxidation is not carried out under equilibrium conditions. We were not able to quantify this experiment due to the intrusion of a slow (> 20 min) decay process, preventing the acquisition of unequivocal equilibrium data at much longer times.

4. Conclusion

The comparatively low potentials required to polymerize terthiophene allow one to deposit films at controlled doping levels. A second consequence of these conditions is the entrapment of incompletely polymerized material within the polymer film. General evidence for the presence of these species comes from the presence of additional features on voltammograms during subsequent potential cycling in monomer-free solution. Evaluation of the additonal charge passed shows that these species comprise up to 20% of the surface immobilized material. Spectroscopic observation of the film during this process allows the direct identification of one of these species as monomer; the remainder is a variety of short chain oligomeric species. An increase in the absorbance associated with polymer accompanies the decrease in absorbance associated with these trapped species upon potential cycling. This demonstrates completion of polymerization occurs during subsequent potential cycling.

Once these irreversible processes are complete, we can investigate the potential dependence of the polymer redox composition. In accord with the observations for the parent thiophene and related pyrrole systems, we find that there are appreciable charging currents associated with polymer oxidation. The inability to separate the faradaic and capacitive contributions to the total current precludes the use of the charge as a means of estimating polymer redox composition. We therefore use the absorbance to estimate the extent of oxidation as a function of potential. Data for the oxidation and reduction processes are different, demonstrating that at least one of these processes is not carried out under equilibrium conditions. In neither case is the composition/potential relationship Nernstian. Given that the doping/undoping process is not a series of simple electron transfers to non-interacting redox sites, this is not surprising.

Acknowledgements

We thank the SERC for equipment grants (GR/C/93622 and GR/D/39399) and RME thanks the SERC for a studentship (88311751).

References

1. J. FEAST and R. FRIEND, *J. Mater. Sci.*, **25** (1990) 3796.
2. G. K. CHANDLER and D. PLETCHER, (Royal Society of Chemistry) "Specialist Periodical Report on Electrochemistry", Vol. 10, (1984) Ch. 3.
3. "Handbook of Conducting Polymers" edited by T. A. Skotheim, (Marcel Dekker, New York, 1986).
4. G. L. BAKER, in "Electronic and Photonic Applications of Polymers" edited by M. J. Bowden and S. R. Turner, ACS Advances in Chemistry Series, Vol. 218, (American Chemical Society, Washington, 1988), p. 271 *et seq.*
5. "Conducting Polymers: Special Applications", edited by L. Alcacer. Proceedings of the Workshop held at Sintra, Portugal, 28–31 July, 1986. (Reidel, Dordrecht, 1987) p. 216.
6. M. FLEISCHMANN and H. R. THIRSK, in "Advances in Electrochemistry and Electrochemical Engineering", edited by P. Delahay. Vol. 3 (Wiley Interscience, New York, 1963) p. 123.
7. S. ASAVAPIRIYANONT, G. K. CHANDLER, G. A. GUNAWARDENA and D. PLETCHER, *J. Electroanal. Chem.* **177** (1984) 229.
8. *Idem, ibid.* **177** (1984) 245.
9. A. R. HILLMAN and E. F. MALLEN, *ibid.* **220** (1987) 351.
10. A. R. HILLMAN and M. J. SWANN, *Electrochim. Acta.* **33** (1988) 1303.
11. W. R. HEINEMAN, F. M. HAWKRIDGE and H. N. BOUNT, in "Electroanalytical Chemistry", edited by A. J. Bard. Vol. 13, (Marcel Dekker, New York, 1984) p. 1.
12. Southampton Electrochemistry Group, "Instrumental Methods in Electrochemistry", (Ellis Horwood Ltd., Chichester, 1985) p. 317.
13. A. R. HILLMAN and E. F. MALLEN, *J. Electroanal. Chem.* **243** (1988) 403.
14. A. HAMNETT and A. R. HILLMAN, *Ber. Bunsenges. Phys. Chem.* **91** (1987) 329.
15. A. HAMNETT and A. R. HILLMAN, *J. Electrochem. Soc.* **135** (1988) 2517.
16. A. J. DOWNARD and D. PLETCHER, *J. Electroanal. Chem.* **206** (1986) 147.
17. J. RONCALI, F. GARNIER, M. LEMAIRE and R. GARREAU, *Synth. Metals* **15** (1986) 323.
18. M. A. DRUY and R. J. SEYMOUR, *J. Phys.* **C3** (1983) 595.
19. B. L. FUNT and S. V. LOWEN, *Synth. Metals* **11** (1985) 129.
20. J. HEINZE, K. HINKELMANN, M. DIETRICH and J. MORTENSEN, *DECHEMA Monographien* **102** (1986) 209.
21. J. RONCALI, M. LEMAIRE, R. GARREAU and F. GARNIER, *Synth. Metals.* **18** (1987) 139.

22. Y. FURUKAWA, M. AKIMOTO and I. HARADA, *ibid.* **18** (1987) 151.
23. Y. YUMOTO, K. MORISHITA and S. YOSHIMURA, *ibid.* **18** (1987) 203.
24. L. LAGUREN-DAVIDSON, C. V. PHAM, H. ZIMMER, H. B. MARK and D. J. ONDRUS, *J. Electrochem. Soc.* **135** (1988) 1406.
25. D. D. CUNNINGHAM, A. GALAL, C. V. PHAM, E. T. LEWIS, A. BURKHARDT, L. LAGUREN-DAVIDSON, A. NKANSAH, O. Y. ATAMAN, H. ZIMMER and H. B. MARK, *ibid.* **135** (1988) 2750.
26. Y. YUMOTO and S. YOSHIMURA, *Synth. Metals* **13** (1986) 185.
27. A. R. HILLMAN and R. M. EALES, *J. Electroanal. Chem.* **250** (1988) 219.
28. J. W. SEASE and L. ZECHMEISTER, *J. Amer. Chem. Soc.* **69** (1947) 271.
29. D. T. SAWYER and J. L. ROBERTS, "Practical Electrochemistry for Chemists" (Wiley Interscience, New York, 1974) p. 77.
30. A. F. DIAZ, J. CROWLEY, J. BARGON, G. P. GARDINI and J. B. TORRANCE, *J. Electroanal. Chem.* **121** (1981) 355.
31. S. W. FELDBERG, *J. Amer. Chem. Soc.* **106** (1984) 4671.
32. R. A. BULL, F. -R. F. FAN and A. J. BARD, *J. Electrochem. Soc.* **129** (1982) 1009.
33. N. MERMILLIOD, J. TANGUY and F. PETIOT, *ibid.* **133** (1986) 1073.
34. J. TANGUY, N. MERMILLIOD and M. HOCLET, *ibid.* **134** (1987) 795.
35. S. N. HOIER, D. S. GINLEY and S. -M. PARK, *ibid.* **135** (1988) 91.

Received 13 June
and accepted 29 June 1989